ISSN 1674-1056
http://cpb.iphy.ac.cn
http://iopscience.iop.org/cpb
中国物理 B
Chinese Physics
中国物理 Chinese Physics B

Accurate capacitance-voltage characterization of organic thin films with current injection

Ming Chu(褚明), Shao-Bo Liu(刘少博), An-Ran Yu(蔚安然), Hao-Miao Yu(于浩淼), Jia-Jun Qin(秦佳俊), Rui-Chen Yi(衣睿宸), Yuan Pei(裴远), Chun-Qin Zhu(朱春琴), Guang-Rui Zhu(朱光瑞), Qi-Zeng(曾琪), and Xiao-Yuan Hou(侯晓远)

Citation: Chin. Phys. B, 2021, 30 (**8**): 087301. DOI: 10.1088/1674-1056/abe3e4
Journal homepage: http://cpb.iphy.ac.cn; http://iopscience.iop.org/cpb

What follows is a list of articles you may be interested in

Method of evaluating interface traps in Al_2O_3/AlGaN/GaN high electron mobility transistors

Si-Qin-Gao-Wa Bao(包斯琴高娃), Xiao-Hua Ma(马晓华), Wei-Wei Chen(陈伟伟), Ling Yang(杨凌), Bin Hou(侯斌), Qing Zhu(朱青), Jie-Jie Zhu(祝杰杰), Yue Hao(郝跃)

Chin. Phys. B, 2019, 28 (**6**): 067304. DOI: 10.1088/1674-1056/28/6/067304

Effect of SiN: H_x passivation layer on the reverse gate leakage current in GaN HEMTs

Sheng Zhang(张昇), Ke Wei(魏珂), Yang Xiao(肖洋), Xiao-Hua Ma(马晓华), Yi-Chuan Zhang(张一川), Guo-Guo Liu(刘果果), Tian-Min Lei(雷天民), Ying-Kui Zheng(郑英奎), Sen Huang(黄森), Ning Wang(汪宁), Muhammad Asif, Xin-Yu Liu(刘新宇)

Chin. Phys. B, 2018, 27 (**9**): 097309. DOI: 10.1088/1674-1056/27/9/097309

Analysis of the inhomogeneous barrier and phase composition of W/4H-SiC Schottky contacts formed at different annealing temperatures

Sheng-Xu Dong(董升旭), Yun Bai(白云), Yi-Dan Tang(汤益丹), Hong Chen(陈宏), Xiao-Li Tian(田晓丽), Cheng-Yue Yang(杨成樾), Xin-Yu Liu(刘新宇)

Chin. Phys. B, 2018, 27 (**9**): 097305. DOI: 10.1088/1674-1056/27/9/097305

Improvement of green InGaN-based LEDs efficiency using a novel quantum well structure

Yangfeng Li(李阳锋), Yang Jiang(江洋), Junhui Die(迭俊珲), Caiwei Wang(王彩玮), Shen Yan(严珅), Ziguang Ma(马紫光), Haiyan Wu(吴海燕), Lu Wang(王禄), Haiqiang Jia(贾海强), Wenxin Wang(王文新), Hong Chen(陈弘)

Chin. Phys. B, 2017, 26 (**8**): 087311. DOI: 10.1088/1674-1056/26/8/087311

Effect of PECVD SiN_x/SiO_yN_x-Si interface property on surface passivation of silicon wafer

Xiao-Jie Jia(贾晓洁), Chun-Lan Zhou(周春兰), Jun-Jie Zhu(朱俊杰), Su Zhou(周肃), Wen-Jing Wang(王文静)

Chin. Phys. B, 2016, 25 (**12**): 127301. DOI: 10.1088/1674-1056/25/12/127301

Accurate capacitance–voltage characterization of organic thin films with current injection*

Ming Chu(褚明)[1], Shao-Bo Liu(刘少博)[1], An-Ran Yu(蔚安然)[2,†], Hao-Miao Yu(于浩淼)[3], Jia-Jun Qin(秦佳俊)[4], Rui-Chen Yi(衣睿宸)[1], Yuan Pei(裴远)[1], Chun-Qin Zhu(朱春琴)[1], Guang-Rui Zhu(朱光瑞)[1], Qi Zeng(曾琪)[5], and Xiao-Yuan Hou(侯晓远)[1,‡]

[1] *State Key Laboratory of Surface Physics, Fudan University, Shanghai* 200433, *China*
[2] *State Key Laboratory of ASIC and System, Center of Micro-Nano System, SIST, Fudan University, Shanghai* 200433, *China*
[3] *Key Laboratory of Luminescence and Optical Information, Ministry of Education, School of Science, Beijing Jiaotong University, Beijing* 100044, *China*
[4] *Department of Physics, Chemistry and Biology (IFM), Linköping University, Linköping SE*-581 83, *Sweden*
[5] *School of Material Engineering, Shanghai University of Engineering Science, Shanghai* 201620, *China*

(Received 23 December 2020; revised manuscript received 27 January 2021; accepted manuscript online 7 February 2021)

To deal with the invalidation of commonly employed series model and parallel model in capacitance–voltage (*C*–*V*) characterization of organic thin films when current injection is significant, a three-element equivalent circuit model is proposed. On this basis, the expression of real capacitance in consideration of current injection is theoretically derived by small-signal analysis method. The validity of the proposed equivalent circuit and theoretical expression are verified by a simulating circuit consisting of a capacitor, a diode, and a resistor. Moreover, the accurate *C*–*V* characteristic of an organic thin film device is obtained *via* theoretical correction of the experimental measuring result, and the real capacitance is 35.7% higher than the directly measured capacitance at 5-V bias in the parallel mode. This work strongly demonstrates the necessity to consider current injection in *C*–*V* measurement and provides a strategy for accurate *C*–*V* characterization experimentally.

Keywords: current injection, organic thin film, capacitance–voltage, parasitic resistance

PACS: 73.23.Ra, 73.61.Le, 84.37.+q, 73.40.Cg **DOI:** 10.1088/1674-1056/abe3e4

1. Introduction

With the advantage of being sensitive to the number of carriers within device and their spatial distribution simultaneously, the capacitance technique has been widely adopted in the study of organic thin films (including organic photovoltaics, organic light-emitting diodes, *etc*.) to probe device properties such as carrier mobility,[1–11] doping density,[12,16] deep trap states,[17–21] and exciton behavior.[22,23] However, rather than the direct obtainment of capacitance, the magnitude and phase of impedance are firstly measured with an LCR meter, subsequently the capacitance of device is calculated according to the circuit model selected.[24,25] Therefore, of upmost importance in maintaining the reliable and accurate capacitance measurement is the selection of a proper circuit model. The series model (consisting of a capacitance C and a parasitic resistance R_S in series, highlighted by the blue box in Fig. 1(a)) and the parallel model (consisting of a capacitance C and a parasitic resistance R_P in parallel, highlighted by the red box in Fig. 1(a)) are two typical equivalent circuit models in capacitance measurement,[24–27] between which, the parallel model is more commonly employed in organic thin films since the series resistance R_S is negligible compared with the parallel resistance R_P (sufficiently high) and the capacitive impedance in a usual measuring frequency range from 10 Hz to 100 kHz.[24,25] However, when the measuring frequency is high enough (exceeding 100 kHz), the capacitive impedance decreases reciprocally with the increase of measurement frequency and drops down to hundreds of Ω or less, the parallel resistance R_P becomes negligible while the existence of series resistance R_S (with a typical value approaching to 100 Ω in organic devices)[25] can significantly influence the measured capacitance according to the parallel model. At the moment, series model is more accurate approximation at high frequency when R_S is a considerable voltage divider, as Carr *et al.* have already discussed.[24] However, in the real *C*–*V* characterization of organic thin film device, the considerable current injection under sufficient bias can also significantly influence the accuracy of measured capacitance in both series and parallel models. Because the parallel resistance R_P (representing the differential resistance of organic thin film, *i.e.* $\mathrm{d}V/\mathrm{d}I$ in *I*–*V* characteristics) dramatically decreases from over 1 MΩ to less than 100 Ω under considerable current injection even at low measuring frequency, at the moment, both the series resistance R_S and the parallel resistance R_P are nonnegligible. The commonly employed series model and parallel model are both

*Project supported by the National Natural Science Foundation of China (Grant Nos. 11874007 and 12074076).
†Corresponding author. E-mail: 12110190029@fudan.edu.cn
‡Corresponding author. E-mail: xyhou@fudan.edu.cn
© 2021 Chinese Physical Society and IOP Publishing Ltd

invalid. But in fact, owing to the lack of an effective method to eliminate the influence of current injection in *C*–*V* characterization, most of researchers regard the measured capacitance in parallel model as a real value of device directly even in large injection condition.[4,26–30]

In this work, with consideration of the current injection within the device, a circuit model consisting of a capacitance (C), an invariable series resistance (R_{S0}), and a nonlinear parallel resistance (R_{Pnl}) is proposed (see Fig. 1(b)). Based on such a model, the relationship between the real capacitance of device and measured items (the experimentally measured capacitance, value of R_{S0}, direct current (DC) differential resistance of the device) is derived theoretically *via* small-signal analysis method. The *C*–*V* measurement on a simulating circuit consisting of a resistor, a diode and a capacitor is performed to verify the theoretical result. Moreover, the real *C*–*V* characteristic of an organic thin film (ITO/pentacene(120 nm)/Al) in consideration of current injection is obtained *via* the theoretical correction of the experimental measurement result, the real capacitance of device is 35.7% higher than the directly measured capacitance at 5-V bias. Our work discovers a common source of deviation in the capacitance measurement of organic devices, which has a significant influence but is rarely studied, and a quantitative method is proposed to correct this deviation. The method eliminates the influence of series parasitic resistance on the capacitance measurement under large DC injection, and is verified to be the only applicable method for organic semiconductor devices to our knowledge.

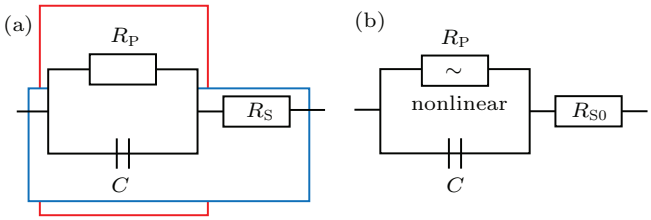


Fig. 1. (a) Small-signal equivalent circuit, with series model highlighted by blue box and parallel model by red box. (b) Equivalent circuit proposed in this work, with an invariable R_{S0} and nonlinear R_{Pnl}.

2. Experimental methods

Organic thin film device studied in this work was fabricated on a commercially pre-etched indium-tin-oxide (ITO)/glass substrate, and the resistance of the ITO anode was less than 17 Ω/square. A 120-nm-thick pentacene layer and a 100-nm-long Al cathode were thermally evaporated on the substrate sequentially. In the evaporation process, the chamber pressure was less than 10^{-4} Pa. The deposition rate was 1 Å/s for pentacene layer and 4 Å/s for Al cathode, respectively. A 3 mm×3 mm active area of device was formed through a shadow mask. The current–voltage (*I*–*V*) measurement, capacitance–frequency (*C*–*F*) measurement, and *C*–*V* measurement were conducted in air on the unencapsulated device immediately after the fabrication process, all measurements were completed within an hour and the measurement results were reproducible. The *I*–*V* measurement was conducted with a Keithley 236 source measure unit (SMU) while the capacitance (both *C*–*V* and *C*–*F*) measurements in parallel mode (with parallel model as the default) were conducted with a programmed HP 4284A LCR meter. The amplitude of the alternating current (AC) signal was set to be 50 mV, the frequency 1 kHz if additional special instruction was absent. The forward bias is defined as a positive potential of the ITO anode.

3. Results and discussion

The capacitance of organic thin film is typically obtained *via* the alternating current (AC) impedance analysis method with an LCR meter.[31] That is, a constant bias (V_0) and a small amplitude modulated AC voltage ($V_1 e^{i\omega t}$) are applied the device simultaneously, the AC impedance ($\tilde{Z}$) or admittance ($\tilde{Y}$) can be obtained experimentally. Typically, according to the selected equivalent circuit of either parallel model (with expression $\tilde{Y} = i\omega C_p + (1/R_P)$, C_P, and R_P are capacitance and parallel resistance) or series model (with expression $\tilde{Z} = (1/i\omega C_S) + R_S$, C_S and R_S are capacitance and series resistance) in LCR meter, the measured capacitance of device can thus be calculated and output automatically.

Specifically, in the *C*–*V* characterization of real organic thin films, the series resistance R_S (mostly originating from the resistance of transparent electrode in organic thin film devices, *e.g.*, ITO) is almost constant, while the parallel resistance R_P (representing the differential resistance dV/dI of organic thin film due to current flowing through the device) strongly depends on the current (or bias) in device. The capacitive impedance is dozens of kΩ under the most commonly employed measurement frequency around 1 kHz in organic thin films. When the current injection is negligible (far less than 1 mA), R_P is sufficiently high and thus parallel model gives accurate capacitance of device. However, when the injected current is considerable, R_P drastically decreases from *c.a.* 1 MΩ (with device current around 1 μA) to less than 1 kΩ (with device current over 1 mA). Comparing R_P with typical R_S approximately 100 Ω in organic thin film device, the influence of R_S is nonnegligible under the significant current injection. Apparently, neither series model nor parallel model is valid at the moment. The discrepancy between the measured capacitance and the real one is closely related to the value of R_S and the differential resistance of device (R_P). Consequently, the effects of R_S and R_P both have to be carefully considered in the equivalent circuit.

3.1. Theoretical derivation of C with small-signal analysis

In principle, an equivalent circuit with both R_S and R_P has more accurate approximation than commonly employed series model or parallel model because the effect of current injection is considered. First of all, the expression of measured capacitance is quantitatively studied in theory according to the equivalent circuit with small-signal analysis method. For an organic thin film device with obvious current injection, a reasonable equivalent circuit is proposed as shown in Fig. 1(b). The organic thin film can be regarded as a DC conductive capacitor, that is, a combination of a nonlinear resistance (R_{Pnl}) and a capacitor (C) in parallel. The R_{S0} can be regarded as an invariable series resistance which mostly originates from the resistance of ITO anode. The $I_0(V)$ and the I–V characteristic of the whole device are obtained directly with a Keithley 236 SMU. It is notable that the voltage V is summation of partial voltage on R_S and the voltage on the organic thin film.

The voltage $\tilde{V}$ applied to the device is

$$\tilde{V} = V_0 + \tilde{V}_1 \mathrm{e}^{\mathrm{i}\omega t}, \tag{1}$$

where V_0 is a constant bias and $\tilde{V}_1 \mathrm{e}^{\mathrm{i}\omega t}$ is the AC voltage with real amplitude V_1 and frequency ω. Accordingly, the current flowing through the device is

$$\tilde{I} = I_0 + \tilde{I}_1 \mathrm{e}^{\mathrm{i}\omega t}. \tag{2}$$

The AC admittance is the ratio of alternating current $\tilde{I}_1$ to the AC voltage $\tilde{V}_1$.

The voltage applied to the capacitor, as well as the nonlinear R_{Pnl} is

$$\tilde{V}' = V_0' + \tilde{V}_1' \mathrm{e}^{\mathrm{i}\omega t}. \tag{3}$$

The AC current flowing through the capacitor C is

$$\tilde{I}_C = \frac{\mathrm{d}\tilde{Q}}{\mathrm{d}t} = \frac{\mathrm{d}\left(C\tilde{V}'\right)}{\mathrm{d}t} = \mathrm{i}\omega C \tilde{V}_1' \mathrm{e}^{\mathrm{i}\omega t}. \tag{4}$$

It is assumed that the measurement frequency is low enough for the charge response of capacitor plates to the AC voltage.

Suppose that the I–V response of nonlinear R_{Pnl} is $I_g(V)$, then the alternating current in R_{Pnl} will be

$$\begin{aligned} \tilde{I}_g &= I_g\left(\tilde{V}'\right) = I_g\left(V_0' + \tilde{V}_1' \mathrm{e}^{\mathrm{i}\omega t}\right) \\ &= I_g\left(V_0'\right) + \frac{\mathrm{d}I_g}{\mathrm{d}V_0'} \tilde{V}_1' \mathrm{e}^{\mathrm{i}\omega t}. \end{aligned} \tag{5}$$

Here, the measurement frequency is assumed to be so low that the I–V characteristic $I_g(V)$ of R_{Pnl} is still valid although the AC voltage is applied. Besides, $I_g\left(\tilde{V}'\right)$ is expanded according to the definition of derivative since $\tilde{V}_1'$ is a small quantity.

Combining Eq. (4) with Eq. (5) yields

$$\tilde{I} = \tilde{I}_C + \tilde{I}_g = I_g\left(V_0'\right) + \left(\mathrm{i}\omega C + \frac{\mathrm{d}I_g}{\mathrm{d}V_0'}\right) \tilde{V}_1' \mathrm{e}^{\mathrm{i}\omega t}. \tag{6}$$

Under DC voltage, no current flowing through the capacitor under steady condition, thus,

$$I_g\left(V_0'\right) = I_0\left(V_0\right). \tag{7}$$

According to the series circuit,

$$V_0 = V_0' + I_0 R_{s0}, \tag{8}$$

$$\tilde{V}_1 = \tilde{V}_1' + \tilde{I}_1 R_{s0}. \tag{9}$$

Taking the derivative Eq. (8) with respect to V_0' gives

$$\frac{\mathrm{d}V_0}{\mathrm{d}V_0'} = 1 + \frac{\mathrm{d}I_0}{\mathrm{d}V_0} \frac{\mathrm{d}V_0}{\mathrm{d}V_0'} R_{s0}. \tag{10}$$

That is,

$$\frac{\mathrm{d}V_0}{\mathrm{d}V_0'} = \frac{1}{1 - \dfrac{\mathrm{d}I_0}{\mathrm{d}V_0} R_{s0}}. \tag{11}$$

Thus,

$$\frac{\mathrm{d}I_g}{\mathrm{d}V_0'} = \frac{\mathrm{d}I_g}{\mathrm{d}V_0} \frac{\mathrm{d}V_0}{\mathrm{d}V_0'} = \frac{\mathrm{d}I_0}{\mathrm{d}V_0} \frac{\mathrm{d}V_0}{\mathrm{d}V_0'} = \frac{\dfrac{\mathrm{d}I_0}{\mathrm{d}V_0}}{1 - \dfrac{\mathrm{d}I_0}{\mathrm{d}V_0} R_{s0}}. \tag{12}$$

Combining Eqs. (6), (9), and (12) together presents

$$\begin{aligned} \tilde{I} &= I_0 + \tilde{I}_1 \mathrm{e}^{\mathrm{i}\omega t} \\ &= I\left(V_0\right) + \left[\mathrm{i}\omega C + \frac{I_0'\left(V_0\right)}{1 - I_0'\left(V_0\right) R_{s0}}\right] \\ &\quad \times \left(\tilde{V}_1 - \tilde{I}_1 R_{s0}\right) \mathrm{e}^{\mathrm{i}\omega t}. \end{aligned} \tag{13}$$

The AC (oscillation) terms are extracted as follows:

$$\begin{aligned} \tilde{Y} &= \frac{\tilde{I}_1}{\tilde{V}_1} = \frac{1}{R_{s0}} \left(1 - \frac{k}{k^2\omega^2 C^2 R_{s0}^2 + 1}\right) \\ &\quad + \mathrm{i} \frac{k^2 \omega C}{k^2 \omega^2 C^2 R_{s0}^2 + 1}, \end{aligned} \tag{14}$$

with

$$k = 1 - I_0'\left(V_0\right) R_{s0}. \tag{15}$$

Comparing with the impedance expression of the parallel model,

$$\tilde{Y} = \mathrm{i}\omega C_p + G_p \tag{16}$$

results in

$$C_p = \frac{\mathrm{Im}\left(\tilde{Y}\right)}{\mathrm{i}\omega} = \frac{k^2}{k^2\omega^2 C^2 R_{s0}^2 + 1} C, \tag{17}$$

$$G_p = \mathrm{Re}\left(\tilde{Y}\right) = \frac{1}{R_{s0}} \left(1 - \frac{k}{k^2\omega^2 C^2 R_{s0}^2 + 1}\right). \tag{18}$$

Equations (17) and (18) are, respectively, the expressions of the measured capacitance and conductance in parallel mode

on the basis of invariable series resistance R_{S0} and DC I–V characteristic $I_0(V_0)$ of the device.

Below discussed are two special limit cases.

(i) When nonlinear R_{Pnl} is sufficiently small, the capacitor is short-circuited, $I_0 = V_0/R_{s0}$, thus $I_0'(V_0) = 1/R_{s0}$ and $k = 0$. Consequently,

$$C_p = 0, \tag{19}$$

$$G_p = \frac{1}{R_{s0}}. \tag{20}$$

Apparently, it is the case of a single series resistance R_{S0}.

(ii) When the resistance of R_{Pnl} is sufficiently high, the direct current within device is negligible, thus $I_0'(V_0)$ approaches 0 and k roughly equals 1. At this time,

$$C_p = \frac{C}{\omega^2 C^2 R_{s0}^2 + 1}, \tag{21}$$

$$G_p = \frac{\omega^2 C^2 R_{s0}}{\omega^2 C^2 R_{s0}^2 + 1}. \tag{22}$$

Equations (20) and (21) give expressions of the capacitance and conductance in the parallel mode under non-current-injection condition, respectively. If $\omega C R_{s0} \ll 1$, then $C_p \approx C$ and $G_p \approx 0$, indicating that the measurement gives the accurate capacitance in parallel mode. Because a typical capacitance of organic thin film device is several nFs, the series resistance is several tens of Ω, thus the deviation of the measured capacitance in parallel mode without current injection is less than 1% as long as the measurement frequency is lower than 100 kHz.

In a real organic thin film device, the series resistance is almost invariable while the I–V characteristic of organic thin film is similar to that of a diode (the resistance keeps large under small bias while decreases rapidly with increasing bias). Therefore, the series resistance R_{S0} is negligible compared with the resistance of organic thin film (R_{Pnl}) under negative bias or small positive bias, similarly in the limit case (ii). With bias increasing, the resistance of organic thin film (R_{Pnl}) decreases rapidly, leading $I_0'(V_0)$ to increase and k to decreases from 1 to 0 gradually, finally similarly in the limit case (i).

3.2. Experimental verification with simulating circuit

To test the accuracy of theoretical capacitance expression with current injection (Eq. (17)), verification experiment should be conducted. Owing to the fact that the multiple factors (free carriers, space charges and traps states)[1–21] affects the device capacitance significantly, the effect of current injection on measured capacitance is difficult to observe *via* the direct C–V measurement in a real organic thin film. Instead, a simulating circuit comprised of three electronic components (a resistor, a capacitor and a diode) is constructed and studied. The series resistance R_{S0} of the whole device is between 40 Ω and 80 Ω experimentally, thus a fixed resistor of 51 Ω is employed as R_{S0} in the simulating circuit. The nonlinear resistance R_{Pnl} is substituted by a 1N4148 type switching diode in the simulating circuit. The response time of the diode is several nanoseconds, which is negligible in C–V measurement with an AC frequency of 1 kHz. The current of the diode is 150 mA at 1-V bias. Although the capacitance of a typical organic thin film is several nFs, a capacitor of about 1 μF is used in the simulating circuit because −0.2 nF for the resistor and −10 nF for the switching diode (at 1-V bias) are detected with an LCR meter. The measured negative capacitance is probably caused by parasitic inductance within electronic components. The real capacitance of the capacitor is 1.017 μF experimentally, more than two orders of magnitude larger than the capacitance of the resistor and switching diode. The conductance of the capacitor is about 5×1^{-5} S.

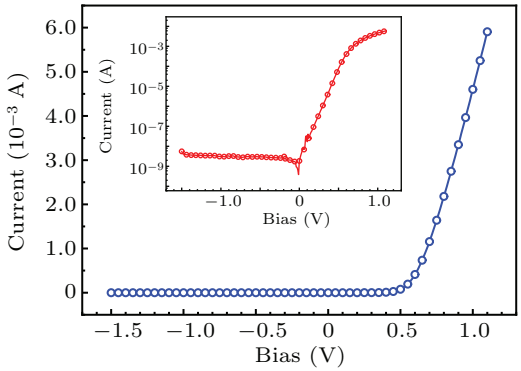


Fig. 2. The I–V characteristic of simulating circuit consisting of a resistor, a switching diode and a capacitor, with inset showing corresponding logarithmic current on y axis.

Firstly, the I–V characteristic of the simulating circuit (of three electronic components) is measured by a Keithley 236 SMU, the result is shown in Fig. 2, where the inset shows the logarithmic current on the y axis. Under negative bias, the current is less than 10^{-8} A while under positive bias, the current increases rapidly with bias increasing, the current exceeds 5 mA at 1.1 V. Moreover, when positive bias is less than 0.75 V, the current increases exponentially with bias increasing as clearly shown in the inset. In such a case, the current is determined dominantly by the diode because its resistance overshadows that of the resistor. When the bias is more than 0.75 V, the I–V characteristic gradually approaches to linear behavior, indicating that the resistance of the diode is obviously less than that of the resistor.

Subsequently, the C–V characteristic of the simulating circuit is shown in Fig. 3. The blue circles in the figure denote experimentally measured result at 1 kHz, the red line refers to the results calculated from Eq. (17). Similarly, the conductance–voltage (G–V) characteristic of the simulating circuit is shown Fig. 1S in the supporting information. In principle, the capacitance of the employed capacitor is bias-independent. However, as clearly indicated in Fig. 3, the measured capacitance in the parallel mode is far less than a real

capacitance value of 1.017 μF, manifesting the inaccuracy of parallel model under significant current injection. In the figure, the capacitance indeed increases drastically at a high bias (over 0.5 V), and the experimental result is well consistent with the theoretical one. Such a consistence strongly confirms the necessity to consider current injection in *C*–*V* measurement, as well as the validity of the above theoretical analysis. Two notes should be mentioned here. 1) The capacitance measured in the simulating circuit under negative bias (at which the current-injection-effect is negligible) is about 0.9 μF, obviously lower than that of the capacitor, this difference can be well explained by the voltage divider of the resistor at 1 kHz. 2) The theoretical capacitance under high negative bias fluctuates and slightly differs from the experimentally measured results. It is because k is very close to 0 at high bias, a slight variation of $I_0'(V_0)$ extracted from the *I*–*V* measurement will cause the value of k to fluctuate drastically.

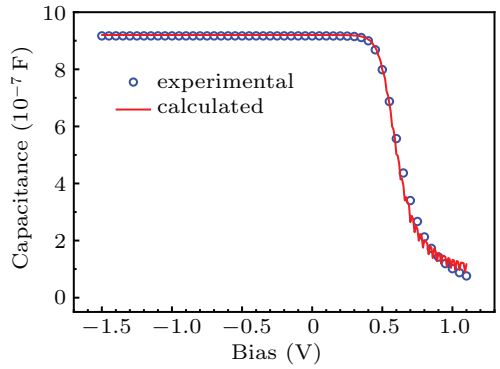


Fig. 3. Experimentally measured (blue circle) and theoretically calculated (red line, according to Eq. (17)) *C*–*V* characteristics of simulating circuit.

3.3. Capacitance correction of real organic thin film device

To further study the influence of current injection on the measured capacitance in a real organic thin film device, holeonly device with the structure of ITO/pentacene (120 nm)/Al (100 nm) is fabricated by thermal evaporation and measured immediately after the fabrication. The *I*–*V* characteristic of the pentacene device is shown in Fig. 4, where inset indicates its logarithmic current on the y axis.

As shown in Fig. 4, the *I*–*V* characteristic indicates obvious rectification property, that is, the current under the positive bias is significantly higher than that under the negative bias. The device current is over 10^{-3} A at 5-V bias, nearly five orders of magnitude higher than the current at −5-V bias. Such rectification is determined by the energy level of material. Hole current can easily be injected from ITO under the positive bias because the highest occupied molecular orbital (HOMO) of pentacene is very close to the Fermi level of ITO, while both electron carriers and hole carriers can be hardly injected under the negative bias because the injection barrier for either electrons or holes is high enough. Thus, only hole current can flow from ITO anode to Al cathode under the positive bias.

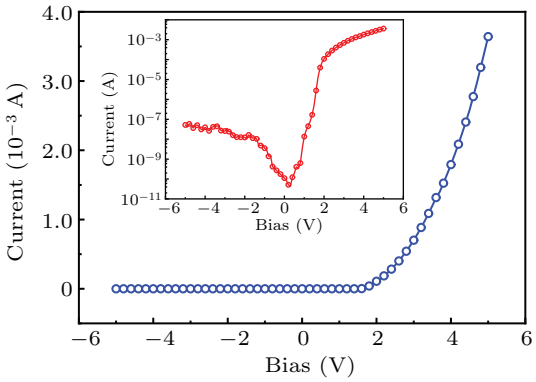


Fig. 4. DC *I*–*V* characteristic of ITO/pentacene (120 nm)/Al device with inset indicating the corresponding logarithmic current on y axis.

The directly measured *C*–*V* characteristic of the pentacene device is shown in Fig. 5 as indicated by blue circles. The measured capacitance is kept constant (about 3.52 nF) under negative bias, this value is basically the geometric capacitance of device because both carriers can hardly be injected into the pentacene layer and the device is quite similar to a parallel-plate capacitor. Under positive bias, capacitance increases rapidly and a sharp peak with a peak value of 15.8 nF appears at 1.7 V. Further increasing the positive bias applied, the capacitance continues to increase and tends to be saturated at 5 V. A higher positive bias can damage the device, so the measuring range is set to be from −5 V to 5 V. Such a capacitance increment under the positive bias possibly originates from trap states, free carriers[29] or space-charge-effect of the injected holes in pentacene.[32]

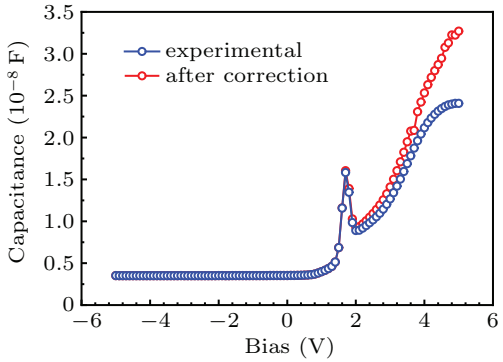


Fig. 5. The *C*–*V* characteristics of ITO/pentacene (120 nm)/Al device. Blue circles refer to experimentally measured capacitance and red squares denote corrected capacitance in consideration of current-injection-effect by the proposed theoretical strategy (according to Eqs. (15) and (17)).

As pointed in Subsection 3.1, the real *C*–*V* response of device could be calculated as long as experimentally measured *C*–*V* characteristic in parallel mode, the DC *I*–*V* characteristic of device and the series resistance were known. The series resistance of device can be extracted from the *C*–*F* measurements at 0 V (see Fig. S2 in the supporting information). The series resistance (R_{S0}) of the pentacene device is 62.5 Ω. Based on the above information, the real *C*–*V* response of the

pentacene device is derived from Eqs. (15) and (17) as shown by red squares in Fig. 5.

Figure 5 shows that the capacitance before and after theoretical correction are almost the same in the range from −5 V to about 2 V where current injection is negligible (see Fig. 4). For the range of 2 V to 5 V, the difference between the corrected capacitance and the measured capacitance grows gradually. At 5-V bias, the capacitance is 24.1 nF for the measured value and 32.7 nF for the corrected value. The real capacitance after correction is about 35.7% higher than the directly measured capacitance in the parallel mode by using an LCR meter. The measured capacitance is greatly influenced by the current injected under the positive bias, and obviously the measured capacitance is no longer accurate. It indicates that the directly measured capacitance in the parallel mode severely deviates from the real value when a considerable current is injected into the device (the differential conductance of the organic thin film is high), even if the measuring frequency is relatively low.

Additionally, the *C*–*V* characteristic based on dual-frequency technique is also calculated and shown in Fig. S3 in the supporting information.[33,34] In the field of inorganic semiconductors, the dual-frequency technique has been used to determine the depletion capacitance in Schottky-barrier device[33] and MOS capacitance[34] with the equivalent circuit model of three elements. The *C*–*V* measurements at two different frequencies yield four equations containing the impedance results, thus the values of C, R_S, and R_P can be extracted. Since this technique can effectively eliminate the influence of parasitic resistance in the capacitance measurement of inorganic semiconductor devices, we investigate whether this method can directly be applied to our organic device. However, as shown in Fig. S3, the *C*–*V* characteristics calculated based on the different combinations of frequencies significantly differ from each other, indicating that this technique is not applicable here. Of particular note is the prerequisite of dual-frequency technique that the capacitance to be measured is frequency independent.[33,34] However, massive researches reveal that the capacitance of organic thin film depends strongly on the measurement frequency.[4,29,32,35,36] Consequently, dual-frequency technique is not valid in organic thin films, and the method we proposed is applicable only for organic devices.

4. Conclusions

In this work, a three-element equivalent circuit comprised of a capacitance (C), an invariable series resistance (R_{S0}), a nonlinear parallel resistance (R_{Pnl}) is proposed. Based on such an equivalent circuit, the expression of the accurate capacitance is derived theoretically in consideration of the current injection within the device. According to the theory, the real *C*–*V* characteristic of device can be calculated from the experimentally measured DC *I*–*V* characteristic, *C*–*V* characteristic, and capacitance–frequency (*C*–*F*) characteristic at 0 V. The proposed equivalent circuit and the theoretical result are verified experimentally by a simulating circuit. Moreover, a real device of organic thin film is fabricated and measured, and its accurate *C*–*V* characteristic is theoretically calculated accordingly. This work strongly demonstrates the necessity to consider the current injection effect in *C*–*V* characterization. For the accurate *C*–*V* characterization of device, a measuring strategy and theoretical correction method are also given. Although the proposed three-element equivalent circuit is more accurate approximation than commonly employed series model or parallel model since the influence of current injection is eliminated, it is still difficult to deal with multiple factors such as free carriers or space charge effect of injected carriers in real devices. A more accurate and powerful equivalent circuit (and related theoretical model) needs to be studied in depth to obtain and investigate the general *C*–*V* characterizations of organic thin films.

References

[1] He Z S, Yu H M, Peng H and Hou X Y 2015 *Chin. Phys. B* **24** 097201
[2] Gong W, Xu Z, Zhao S L, Liu X D, Fan X, Yang Q Q and Kong C 2013 *Chin. Phys. B* **22** 128402
[3] Oklobia O, Komilian S and Sadat-Shafai T 2018 *Org. Electron.* **61** 276
[4] Lee Y S, Park J H and Choi J S 2002 *Opt. Mater.* **21** 433
[5] Li J V, Nardes A M, Liang Z Q, Shaheen S E, Gregg B A and Levi D H 2011 *Org. Electron.* **12** 1879
[6] Lee S H, Lee J H, Kim K H, Yoo S J, Kim T G, Kim J W and Kim J J 2012 *Org. Electron.* **13** 2346
[7] Chen B B, Qiao X F, Liu C M, Zhao C and Chen H C 2013 *Appl. Phys. Lett.* **102** 193302
[8] Garcia-Belmonte G, Munar A, Barea E M, Bisquert J, Ugarte I and Pacios R 2008 *Org. Electron.* **9** 847
[9] Ecker B, Nolasco J C, Pallares J, Marsal L F, Posdorfer J, Paroso J and von Hauf E 2011 *Adv. Funct. Mater.* **21** 2705
[10] Martens H C F, Huiberts J N and Blom P W M 2000 *Appl. Phys. Lett.* **77** 1852
[11] Liu R L, Wang X L and Tang C 2014 *Acta Phys. Sin.* **63** 028105 (in Chinese)
[12] Yu A R, Pei Y, Yi R C, Liu S B, Chu M, Yu H M, Tang Y J, He Z S and Hou X Y 2017 *Org. Electron.* **46** 121
[13] Sharma G D, Saxena D and Roy M S 2001 *Synthetic Met.* **123** 189
[14] Dennler G, Lungenschmied C, Sariciftci N S, Schwodiauer R, Bauer S and Reiss H 2005 *Appl. Phys. Lett.* **87** 163501
[15] Liu Q, He Z Q, Liang C J, Zhao Y, Xiao W K and Li D 2015 *Chin. Phys. Lett.* **32** 056801
[16] Gong W, An T, Liu X Y and Lu G 2019 *Chin. Phys. B* **28** 038501
[17] Takagi K, Nagase T, Kobayashi T and Naito H 2016 *Appl. Phys. Lett.* **108** 053305
[18] Shintaku N, Izawa S, Takagi K, Naito H and Hiramoto M 2017 *Org. Electron.* **50** 515
[19] Boix P P, Garcia-Belmonte G, Munecas U, Neophytou M, Waldauf C and Pacios R 2009 *Appl. Phys. Lett.* **95** 233302
[20] Reis F T, Mencaraglia D, Saada S O, Seguyb I, Oukachmihb M, Jolinatb P and Destruel P. 2003 *Synthetic Met.* **138** 33
[21] Zheng R, Huang W B, Xu W and Cao Y 2014 *Chin. Phys. Lett.* **31** 027703
[22] Yu H M, Yi R C, Li W B, Zhang J W, He Yun, Zeng Q and Hou X Y 2015 *J. Phys. D: Appl. Phys.* **48** 455108
[23] Chu M, Liu S B, Yu A R, Zeng Q, Zhong G Y and Hou X Y 2019 *J. Phys. Chem. C* **123** 17384

[24] Carr J A and Chaudhary S 2012 *Appl. Phys. Lett.* **100** 213902
[25] Yu H M and He Y 2018 *Chin. Phys. B* **27** 067202
[26] Tsai M N, Chang T C, Liu P T, Ko C W, Chen C J and Lo K M 2006 *Thin Solid Films* **498** 244
[27] Kim J M and Kim J J 2019 *Org. Electron.* **67** 43
[28] Li J H, Qiao B, Zhao S L, Song D D, Zhang C W and Xu Z 2020 *Org. Electron.* **83** 105756
[29] Zhang J W, He Y, Chen X Q, Pei Y, Yu H M, Qin J J and Hou X Y 2015 *Org. Electron.* **21** 73
[30] Zhang J W, Qin J J, Yu H M, Chen X Q and Hou X Y 2016 *Org. Electron.* **28** 239
[31] Yu A R, Liu S B, Zeng Q, Yi R C, Yu X X, Hou X Y and Zhong G Y 2019 *J. Appl. Phys.* **126** 204501
[32] von Mensfoort S L M and Coehoorn R 2008 *Phys. Rev. Lett.* **100** 086802
[33] Lonnum J F and Johannessen J S 1986 *Electron. Lett.* **22** 456
[34] Yang K J and Hu C M 1999 *IEEE Electron. Dev.* **46** 1500
[35] Xu H, Tang C, Zhai W J, Liu R L, Rong Z, Fan L Q and Huang W 2014 *Synthetic Met.* **198** 221
[36] Pang H S, Xu H, Tang C, Meng L K, Ding Y, Xiao J, Liu R L, Pang Z Q and Huang W 2019 *Org. Electron.* **65** 275